International Journal of Mass Spectrometry 304 (2011) 195–203

Contents lists available at ScienceDirect

International Journal of Mass Spectrometry

journal homepage: www.elsevier.com/locate/ijms

Assessment of the gas phase stability of quadruplex DNA using travelling wave ion mobility mass spectrometry

Karina C. Porter, Jennifer L. Beck*

School of Chemistry, University of Wollongong, Northfields Avenue, Wollongong, New South Wales 2522, Australia

ARTICLE INFO

Article history:
Received 29 March 2010
Received in revised form 16 October 2010
Accepted 27 October 2010
Available online 4 November 2010

Keywords:
Ion mobility mass spectrometry
Quadruplex DNA
DNA
Electrospray

ABSTRACT

The quadruplex DNA (qDNA) $(dT_2G_5T)_4$, $(dG_4T_4G_4)_2$, and the intramolecular $d[G_3(T_2AG_3)_3]$ (Q4, Q2 and Q1, respectively), were analysed using circular dichroism (CD) spectroscopy and electrospray ionisation travelling wave ion mobility mass spectrometry (ESI-TWIMS). The CD spectra of the three qDNAs showed, in agreement with the literature, that in ammonium acetate, pH 7.0, Q4 exhibited a parallel strand orientation while Q2 and Q1 were predominantly anti-parallel qDNA. At high concentrations of Q2, the CD spectrum was consistent with a mixture of anti-parallel and parallel forms. ESI-travelling wave ion mobility mass spectra of the qDNA sequences were compared under solution conditions where they were known to be stable and under conditions where they were known to be destabilised (low ammonium acetate concentration with acetonitrile present). This comparison enabled the distinction of ions of the same mass-to-charge that corresponded to single-stranded (ss)Q2, $[(dG_4T_4G_4)]$, or bimolecular Q2, $[(dG_4T_4G_4)_2]$. The resolution of the ESI-TWIMS instrument was sufficient to determine that the ions carrying four and five negative charges most likely arose from the folded intramolecular qDNA, Q1, while the ion carrying six negative charges most likely arose from unfolded Q1. This work shows the utility of ESI-TWIMS in distinguishing among different conformations and structures of qDNA.

1. Introduction

The DNA present in cells exists not only as the familiar double-stranded, Watson–Crick H-bonded DNA [1], but also in a range of secondary structures that form as a result of the predisposition of various sequences to form these structures, and as the result of interactions with proteins [2]. For example, single-stranded regions of DNA occur as it is unwound to present a template for replication, Z-DNA and triplex DNA is favoured by some sequences, and Holliday junctions form at recombination sites. Some of the sequences which form triplexes, cruciforms and slipped structures can lead to mutations that underlie neurological, psychiatric and other diseases [3].

Quadruplex DNA (qDNA) is formed when four guanosine residues (G-quartet or G-tetrad) are arranged in a planar structure. Sequences that form qDNA have the general sequence: $G_{3-5}N_{L1}G_{3-5}N_{L2}G_{3-5}N_{L3}G_{3-5}$ where N_{L1-3} are loops that vary in length and sequence [4]. Sequences such as this can fold back upon themselves to produce an intramolecular quadruplex. Depending on the length of the G-rich tracts and the lengths of the loops, the four parts of the strand comprising the quadruplex can be arranged in a parallel or anti-parallel fashion. The loops can be diagonal or lateral and may also contain secondary structure [4 and references therein]. Intermolecular quadruplex structures can also be formed *in vitro* from two or four strands and may be stabilised by the presence of monovalent cations that are present in the centre of the tetrad [5–7].

Human chromosomes contain repeating G-rich, single-stranded sequences, 5′-$d(T_2AG_3)$, of about 150–250 nucleotides at their 3′ ends [8]. These regions are the telomeres [9]. Guanine-rich sequences are also found in gene promoters such as the *c-myc* oncogene [10]. The solution structure of a 24-nucleotide five guanine tract sequence from this gene has been determined in the presence of potassium ions and shows that it has a parallel-stranded G-tetrad core associated with three double-chain reversal loops in addition to other structural features [11]. That qDNA may form in telomeres and in gene promoter regions of DNA is significant as the presence of these structures may have effects on cellular processes such as transcription and the cell cycle itself. The length of the telomeres is maintained by the enzyme telomerase. The observation that telomerase activity is associated with 80–85% of cancer cells but not with normal somatic cells stimulated interest in targeting telomeres and their interactions with proteins for anti-cancer drug development [12]. Overexpression of the *c-myc* gene is associated with the progression of many cancers [10], and it has been suggested that novel therapeutics that target disease-related genes may be developed from small-molecule gene regulators that target qDNA in promoter regions of genes such as *c-myc* [4].

Abbreviations: qDNA, quadruplex DNA; TWIMS, travelling-wave ion mobility mass spectrometry; NH_4OAc, ammonium acetate; ESI, electrospray ionisation.

* Corresponding author. Tel.: +61 2 42 214177; fax: +61 2 42 214287.
E-mail address: jbeck@uow.edu.au (J.L. Beck).

1387-3806/$ – see front matter © 2010 Elsevier B.V. All rights reserved.
doi:10.1016/j.ijms.2010.10.033

The diversity of the qDNA structures that can be formed considering the different lengths of the loops and the length of guanine tracts makes the design of qDNA-selective ligands a challenging task. There are a few compounds which have shown selectivity for different types of qDNA. For example, telomestatin preferentially binds intramolecular over intermolecular quadruplex structures, while TMPyP4 has a greater affinity for intermolecular structures [7]. *In vivo* anti-cancer activity has been observed for telomestatin, the tri-substituted acridine compound, BRACO-19, and the polycyclic RHSP4 [4 and references therein]. In order to screen the binding of small molecules to qDNA, a range of oligonucleotide sequences that form different types of quadruplex for which X-ray crystal structures are available have been studied. These include: tetramolecular sequences (four strands) of the type d(TG_4T) which form a parallel-stranded structure, bimolecular sequences (two strands) of sequences such as d($G_4T_4G_4$), and unimolecular sequences (one strand) where the only example is d[$AG_3(T_2AG_3)_3$] [13 and references therein].

Prior to carrying out binding studies it is important to ensure that folded qDNA is present in solution. Circular dichroism has been used to assess whether qDNA strands are parallel or anti-parallel. Anti-parallel qDNA has a maximum (positive) ellipticity around 295 nm with a negative band near 260 nm while parallel qDNA has a maximum (positive) ellipticity near 265 nm and a negative band near 240 nm [14–16]. While this solution method can confirm the presence of qDNA and enable the assessment of strand orientation, it does not allow determination of strand stoichiometry, for example, whether the qDNA is intra or intermolecular. Electrospray ionisation mass spectrometry (ESI-MS) has been widely applied to test the binding of small molecules to DNA [17–19] and enables precise determinations of stoichiometry. Ambiguities, however, arise in the ESI-MS analysis of bimolecular and tetramolecular qDNA formed from identical strands (identical mass) since, for example, a two-stranded quadruplex with n negative charges will have the same mass to charge ratio (m/z) as a single strand carrying $n/2$ charges. Furthermore, in the analysis of intramolecular single-stranded qDNA it is not possible to determine using ESI-MS whether the strand remains folded in the gas phase as the mass of the unfolded and folded structures is the same. If the qDNA is unfolded in the mass spectrometer, small molecules that were bound in solution may dissociate from the DNA giving a false negative result in drug/DNA binding studies.

Ion mobility mass spectrometry can be used to analyse the gas phase conformations of biomolecules [20]. Bowers and coworkers addressed the issues concerning whether qDNA structures can be maintained in the gas phase by comparing cross-sections of various theoretical structures with cross-sections determined from the experimental arrival time distributions. They investigated different lengths of the human telomeric repeat d$(T_2AG_3)_n$ (where n = 1, 2, 4 and 6) and dTG_4T; in all cases these were matched to model cross-sections with specific strand orientations and structures [16]. This work was extended to include other qDNA structures and qDNA complexes with quinacridine ligands that are telomerase inhibitors as well as the extensively studied TMPyP4 and PIPER [21]. The electrospray drift cell (direct current) ion mobility (DCIM) mass spectrometer used in that work was built in-house [22]. The recent commercial release of an instrument that employs travelling wave (T-wave) ion mobility mass spectrometry (TWIMS) [23] has meant that the ability to carry out ion mobility separations is potentially available to more researchers. In TWIMS, a high electric field is applied to one segment of the mobility cell and swept through the cell one segment at a time in the direction of ion migration [20]. This differs from direct current ion mobility mass spectrometry where a low field is applied continuously to the mobility cell. Data obtained from DCIM mass spectrometry can be used to measure the absolute collisional cross-section of an ion. Cross-sections cannot be determined directly from TWIMS data, but can be obtained from calibration curves obtained using DCIM data; furthermore, the resolution with respect to ion mobility is lower [24]. The potential advantages of the TWIMS instrument are its high sensitivity and the ability to simultaneously collect mass spectra and arrival times of ions [20].

Previously, ESI-MS was used to investigate the selectivity of an indolyl berberine compound for binding to the tetrameric qDNA $(dT_2G_5T)_4$ (called Q1 here) over duplex DNA [25]. As a prelude to investigations of the binding of this compound and its derivatives to other types of qDNA [26], it was important to confirm that the qDNA to be studied was folded in solution and that the structure was maintained in the gas phase. In the current work, TWIMS has been applied to compare the drift times of various types of qDNA sprayed from ammonium acetate solutions in which the various qDNAs were shown by CD to be folded. The qDNA sequences used were the intermolecular tetrameric $(dT_2G_5T)_4$ and bimolecular $(dG_4T_4G_4)_2$, and the intramolecular d[$G_3(T_2AG_3)_3$] (called here Q4, Q2 and Q1, respectively). These or similar sequences have been previously studied by ESI-MS [27,28] and solution or crystal structures are available [13]. Solution conditions were then changed to destabilise the qDNA structures and the solutions were again analysed by TWIMS. Under the new conditions, ions (of the same mass/charge) with new drift times were observed for a bimolecular qDNA (Q2) strongly suggesting that under the original conditions folded, two-stranded qDNA was maintained *in vacuo* and detected. The single strand carrying half the number of charges increased substantially in abundance when the ionic strength was lowered. When the ion mobilities of the intramolecular qDNA (Q1) were compared at relatively high and low ionic strength, a new ion ($[Q1\text{-}6H]^{6-}$) was detected and its mobility suggested that it was from unfolded qDNA. Furthermore, under some conditions ions were observed that were consistent with dimers of Q1 and Q2. These are the first travelling wave ion mobility mass spectra of qDNA sequences. A comprehensive rationale is given for the assignment of ions based on observations of changes in the spectra of the qDNAs sprayed from different solutions. This work highlights the utility of TWIMS in characterising the stoichiometries and conformations of qDNA present in a sample.

2. Experimental

Reagents were of the highest grade commercially available. MilliQ™ water from Millipore (Bedford, USA), was used in all experiments.

2.1. DNA

The oligonucleotides comprising the qDNA Q4, Q2 and Q1: single-stranded (ss)Q4 dT_2G_5T, Q1 d[$G_3(T_2AG_3)_3$] and ssQ2, $dG_4T_4G_4$, were obtained from Geneworks (South Australia) as 'trityl off' derivatives. Note that the names refer to the number of strands that are expected to be present to form qDNA based on X-ray crystal structures [13 and references therein]. For example, the qDNA, Q4, will consist of four strands of dT_2G_5T while Q1 will form a unimolecular quadruplex structure by folding back on itself. HPLC purification of oligonucleotides was performed as previously described [25] and the dried ssDNA was redissolved in water giving concentrations of the stock in the range 0.3–1.0 mM and then stored at −20 °C. Quadruplex DNA was prepared by taking an appropriate volume of each DNA sequence, taking it to dryness using a Savant SpeedVac and redissolving in 0.15 M NH_4OAc, pH 7.0, to give a concentration of 1 mM for quadruplex DNA. The DNA was annealed by heating to 95 °C for 15 min and the solutions were then allowed

Table 1
Mass spectrometry conditions used to acquire ion mobility mass spectra using the Synapt™ HDMS™ (ESI-TWIMS).

Parameter	Value	Parameter	Value
Scan time (s)	3.9	Trap DC bias (V)	28
Scans in driftscope function	200	Trap DC exit (V)	5
Trap pressure (mbar)	2.04e−2	IMS DC entrance (V)	5
IMS pressure (mbar)	4.86e−1	IMS DC exit (V)	2
TOF pressure (mbar)	1.30e−6	Transfer DC entrance (V)	2
Capillary (V)	2100	Transfer DC exit	2
Sampling cone (V)	40	Source wave velocity (m/s)	300
Desolvation temperature (°C)	150	Source wave height (V)	0.2
Trap collision energy (V)	6	Trap wave velocity (m/s)	300
Transfer collision energy (V)	3	Trap wave height (V)	8
IMS gas flow (ml/min)	24	IMS wave velocity (m/s)	350
Trap DC entrance (V)	5	IMS wave height (V)	8
Transfer wave height (V)	3	Transfer wave velocity (m/s)	248

to slowly cool to room temperature. Annealed qDNA was stored at 5 °C.

2.2. Circular dichroism

CD spectra (220–320 nm) were obtained using a Jasco J-810 spectropolarimeter and a 0.1 cm pathlength quartz cell at 25 °C. In some experiments the stability of the DNA was tested by changing solution or instrument conditions. These are described in the relevant sections of the text. The sensitivity was set to standard, data pitch was 0.1 nm, scanning mode was continuous, scanning speed was 100 nm/min, response was 4 s, bandwidth was 1 nm, and accumulation was set to 6 scans.

2.3. ESI-MS and ESI ion mobility mass spectrometry

ESI and ion mobility mass spectra were acquired in negative ion mode using a Waters HDMS™ Synapt™ ESI mass spectrometer (Manchester, UK; called an ESI-TWIMS instrument here). Samples were injected into the source of the mass spectrometer using a Harvard model 22 syringe pump (Natick, MA, USA) at a flow rate of 5 μl/min. The instrument was calibrated using caesium iodide (1 mg/ml) over the same mass range used to acquire spectra. Table 1 shows the different parameters used in order to obtain ion mobility mass spectra of Q4, Q1 and Q2 (spectra shown in Figs. 3–5). In some experiments the spectra were acquired in ESI-MS mode only. In these cases the trap and transfer energies were 4 and 2 V, respectively (spectra not shown). In preliminary experiments to confirm the best conditions for obtaining ESI mass spectra of Q1, Q2 and Q4 a Waters Q-TOF *Ultima* ESI mass spectrometer was used. The capillary was 2.5 kV for all qDNA samples. The cone voltages for Q4, Q1 and Q2 were 150, 80 and 100 V, respectively, and the RF lens 1 voltages were 70, 70 and 45 V.

3. Results and discussion

3.1. ESI mass spectra of Q4, Q1 and Q2

The tetramolecular qDNA used in this study, Q4 $(dT_2G_5T)_4$, is the same sequence that was used by David et al. in an ESI-MS study to investigate the interactions of tetrameric qDNA with the compounds Tel01, distamycin A and diethylthiocarbocyanine [28]. This sequence has also been used in our laboratory to investigate the binding of novel ligands to qDNA [25]. The similar sequence $(dTG_4T)_4$ contains one fewer guanosine residue and has

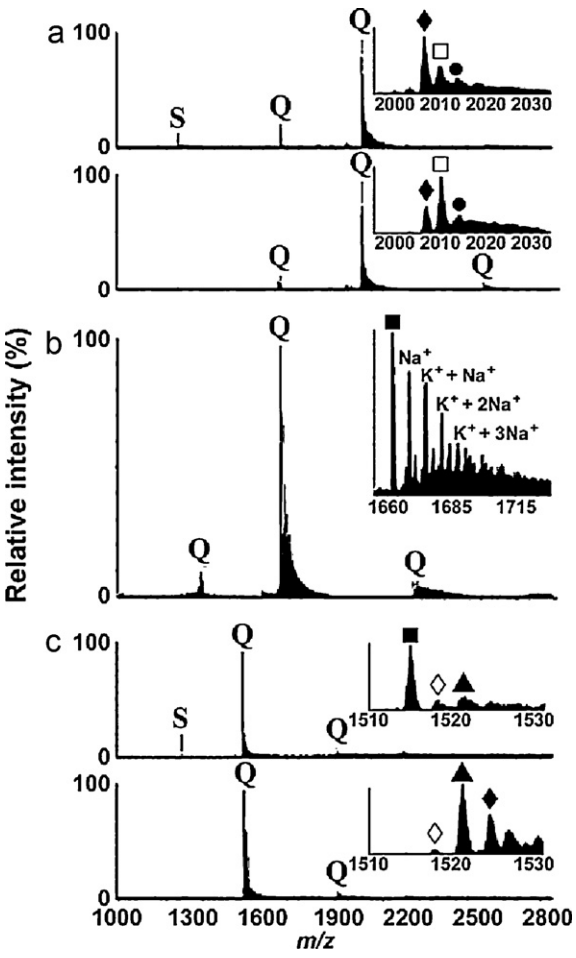

Fig. 1. Negative ion ESI mass spectra of Q4, Q1 and Q2 (pH 7.0) (a) Q4. Top: in 50 mM NH_4OAc. Bottom: in 150 mM NH_4OAc. Insets: view of the *m/z* range 2000–2030. (b) Q1 in 150 mM NH_4OAc. Inset: view of the *m/z* range 1660–1720. (c) Q2 in 150 mM NH_4OAc. Top: RF lens 1 was 70 V. Bottom: RF lens 1 was 45 V. The ions are assigned in the text. Insets: view of the *m/z* range 1510–1530. **S** and **Q** refer to single-stranded DNA and qDNA, respectively. (■) qDNA alone (no adducts); (◊) qDNA + $1NH_4^+$; (▲) qDNA + $2NH_4^+$; (♦) qDNA + $3NH_4^+$; □ qDNA + $4NH_4^+$; (●) qDNA + $5NH_4^+$.

also been investigated by ESI-MS [27], and ESI-MS, ion mobility (DCIM) and molecular dynamics calculations were consistent with the maintenance of a four-stranded parallel-stranded structure in the gas phase [16]. In each of these studies, the mass of the qDNA determined from the negative ion ESI mass spectra revealed that ammonium ions were bound in the quadruplex. In ESI mass spectra of duplex DNA, no ammonium ions are evident as they are present in the solvent only to assist in the ionisation process. In the case of the tetrameric qDNA, the ammonium ions serve to stabilise the guanosine tetrad as has been observed for Na^+ and K^+ in solution studies. Since each strand of Q4 contains a tract of five guanosine residues, it is expected that up to four monovalent cations can be bound in the qDNA structure. Fig. 1(a) shows ESI mass spectra of Q4 obtained in 50 mM (top) and 150 mM NH_4OAc (bottom), pH 7.0, with the *m/z* region 2000–2030 in the insets showing the ammonium ion adducts that were present in the spectra. The most abundant ion in the mass spectra was $[Q4 + 4NH_4^+ - 9H]^{5-}$ at *m/z* 2010.0. This is in agreement with our previous work [25]. When Q4 was sprayed from 50 mM ammonium acetate, some single strands from Q4 (3− and 2− ions at *m/z* 831.2 and 1247.3, respectively) were present. Therefore the tetrameric qDNA is more stable when sprayed from 150 mM NH_4OAc in agreement with earlier work [25,27,28]. Furthermore, the insets show that under this condi-

tion, $[Q4 + 4NH_4^+ - 9H]^{5-}$ is approximately twice as abundant as $[Q4 + 3NH_4^+ - 8H]^{5-}$. The presence of $4NH_4^+$ is consistent with the structure expected when all possible binding sites for monovalent cations inside the qDNA are occupied (4 monovalent cations for 5 guanosine tetrads). It is likely that ammonium ions are lost from the structure in the mass spectrometer. Increasing cone voltages and collision energies applied in experiments using a Waters Q-TOF2 ESI mass spectrometer resulted in dissociation of ammonium ions from the similar qDNA $(dTG_4T)_4$ [27].

Q1 ($d[G_3(T_2AG_3)_3]$) is expected to form an intramolecular qDNA where the single strand folds back upon itself to form the guanosine tetrad comprised of tracts of three contiguous guanines. This sequence has the features of the human telomeric sequence: single-stranded with three guanosine residues, and has been used in a previous ESI-MS study as a model for the human telomere [27]. An X-ray crystal structure of the similar sequence $d[AG_3(T_2AG_3)_3]$ [29], showed that in the presence of K^+, the qDNA was an intramolecular parallel quadruplex. In NMR studies of solutions of this qDNA containing Na^+, an anti-parallel arrangement was observed, while other biophysical methods have suggested that this and similar qDNA exists as a mixture of parallel and anti-parallel qDNA [30,31]. Fig. 1(b) shows the negative ion ESI mass spectrum of Q1 sprayed from 150 mM ammonium acetate, pH 7.0. The most abundant ion was $[Q1\text{-}4H]^{4-}$ at m/z 1662.3. The $[Q1\text{-}5H]^{5-}$ and $[Q1\text{-}3H]^{3-}$ ions were substantially less abundant. The inset in Fig. 1(b) shows an expanded view of the region m/z 1660–1730. While there were no significant ions that could be attributed to NH_4^+ adducts of Q1, there were a substantial number of adducts that were consistent with the presence of bound Na^+ and K^+. A spectrum of Q1 (called Q3 in their study) was obtained by Rosu et al. [27]. They also found that there was no favoured stoichiometry for binding of NH_4^+ to Q1 and under gentle instrument conditions the predominant ions were from Q1 with zero or one NH_4^+ bound. In our hands, Q1 was the only qDNA where significant Na^+ and K^+ adducts were consistently observed. The spectra were repeated on many occasions using different sources of Q1 and the experiments were carried out alongside those using Q2 and Q4. All qDNA was prepared using water and ammonium acetate from the same source, suggesting that Q1, in contrast with Q4 and Q2 (see below) preferentially bound adventitious Na^+ and K^+ that may have been present at low concentrations in the solutions, over NH_4^+. It is perhaps not surprising that different cations might be favoured under certain conditions since different structures of the human telomeric sequence, $d[AG_3(T_2AG_3)_3]$, have been observed in the presence of different cations [13 and references therein].

Q2 is found in the telomere of the ciliated protozoan, *Oxytricha nova*. It forms an anti-parallel qDNA, $(dG_4T_4G_4)_2$, with diagonal loops [32] and an ESI mass spectrum of it has been reported previously [27]. Fig. 1(c) shows the negative ion ESI mass spectra of the intermolecular two-stranded qDNA, Q2 $(dG_4T_4G_4)_2$, sprayed from 150 mM NH_4OAc, pH 7.0, with the RF lens 1 of the Q-TOF *Ultima* mass spectrometer set at 70 V (top) and 45 V (bottom). The ions carrying four negative charges were present in low abundance, but the most abundant of these was $[Q2 + 3NH_4^+ - 7H]^{4-}$ at m/z 1906.0. The most abundant ions were those carrying five negative charges (m/z 1514.4 for $[Q2\text{-}5H]^{5-}$). The insets show the ammonium adducts that were associated with the 5− ion. At the lower RF lens voltage (bottom inset) $[Q2 + 2NH_4^+ - 7H]^{5-}$ at m/z 1521.2 was the most abundant ion with $[Q2 + 3NH_4^+ - 8H]^{5-}$ present at approximately half the abundance. At the higher voltage some ssQ2 was present at low abundance and the major ion from qDNA was from Q2 with no bound ammonium ions. Rosu et al. [27] also observed changes in the number of bound ammonium ions depending on the mass spectrometry conditions.

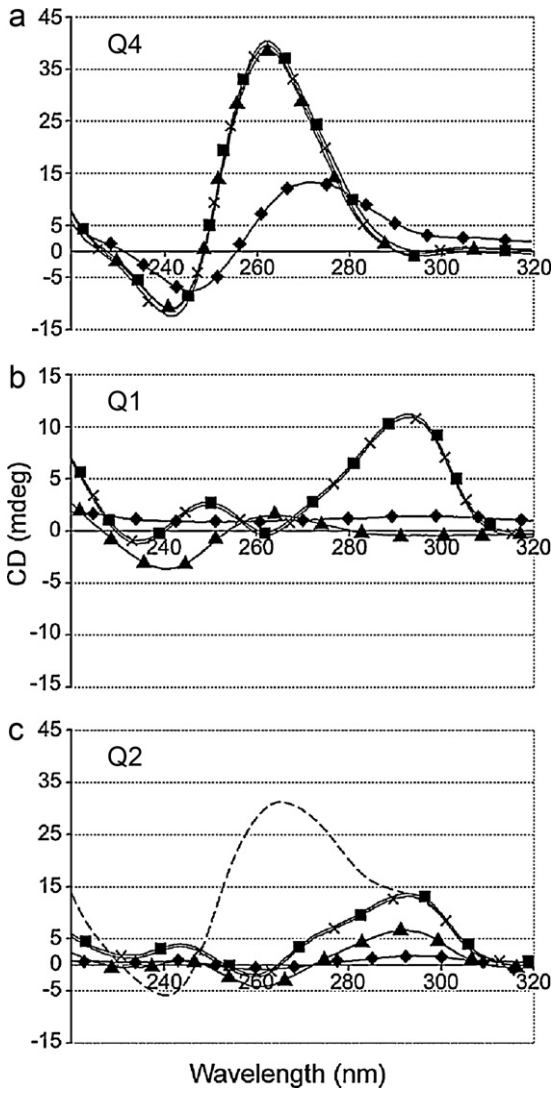

Fig. 2. CD spectra of Q4, Q1 and Q2 under different solution conditions (pH 7.0). (a) Q4 at 20 μM. (b) Q1 at 20 μM. (c) Q2 at 20 μM or 40 μM. (■) In 150 mM NH_4OAc; (×) in 5 mM NH_4OAc; (♦) in 5 mM NH_4OAc, 80% in acetonitrile; (▲) in 150 mM NH_4OAc heated to 80 °C; (- - -) 40 μM Q2 in 150 mM NH_4OAc.

3.2. CD spectra of Q4, Q1 and Q2

The presence of abundant ions carrying an odd number of charges (5) for Q4 and Q2 confirms that the number of strands expected to form qDNA (four for Q4 and two for Q2) were present in non-covalent complexes that were stable in the mass spectrometer. The loss of ammonium ions under some conditions suggests that dissociation occurs when conditions are less gentle and highlights the care that needs to be taken to optimise the conditions. In agreement with other work, no ammonium ions were present in Q1. Since this DNA sequence is expected to form a single-stranded intramolecular qDNA, it is difficult using ESI mass spectra alone to be sure that qDNA was present. In order to obtain supporting evidence for the presence of qDNA in 150 mM NH_4OAc, pH 7.0, in our hands, especially in the case of Q1, and to determine the stability of the various qDNA structures under different solution conditions, CD spectra were obtained.

Fig. 2 shows CD spectra for Q4 (a), Q1 (b) and Q2 (c) under different solution conditions. The CD spectrum of Q4 in 150 mM NH_4OAc had a maximum positive ellipticity at

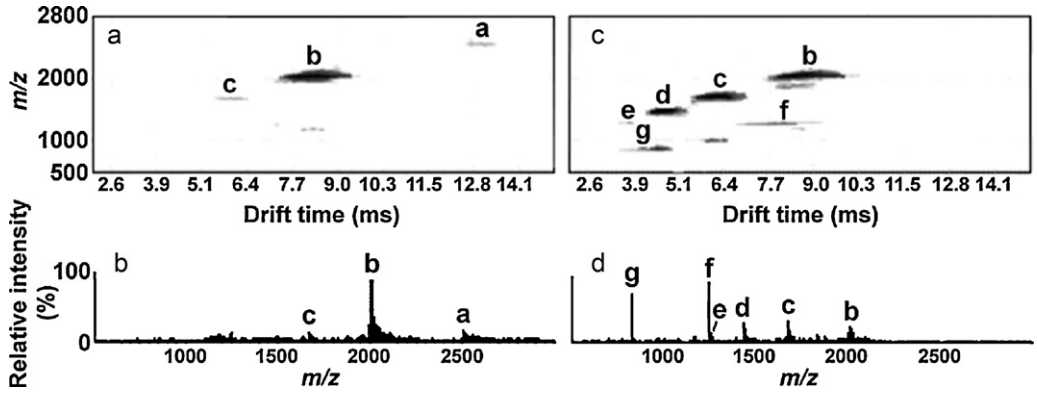

Fig. 3. Negative ion ESI mass spectra and TWIMS driftscope images of Q4. (a), (b) In 150 mM NH_4OAc. (c), (d) In 5 mM NH_4OAc. The ions from intact Q4 are **a–e** which correspond to $[Q4 + 4NH^{4+} - 8H]^{4-}$, $[Q4 + 4NH^{4+} - 9H]^{5-}$, $[Q4 + 4NH^{4+} - 10H]^{6-}$, $[Q4 + 4NH^{4+} - 11H]^{7-}$ and $[Q4 + 4NH^{4+} - 12H]^{8-}$, respectively. All ions are assigned in Table 2.

~260 nm and a minimum (negative) ellipticity at 242 nm consistent with parallel qDNA. The spectrum was unchanged when the solution was heated to 80 °C or when the NH_4OAc concentration was decreased to 5 mM showing that the quadruplex was stable under the conditions. A change in the spectrum was observed when Q4 was in 5 mM NH_4OAc/80% acetonitrile suggesting some disruption of the qDNA may have occurred.

The CD spectrum of Q1 that had been annealed in either 5 mM or 150 mM NH_4OAc, pH 7.0, showed a positive maximum at 295 nm, a minimum at 260 nm and another lower intensity maximum at ~248 nm. This is consistent with an anti-parallel strand orientation [33,15]. This CD spectrum of the annealed Q1 (Fig. 2(b)) is very similar to the spectrum obtained when Na^+ was present in a solution containing the 24 mer sequence in which T_2AG_3 is repeated four times in the one strand [33]. In contrast, in the presence of ammonium ions this sequence has previously given a somewhat different spectrum in which the major features were still a maximum at 295 nm, but there was a shoulder at ~270 nm and the minimum at 260 nm had a positive ellipticity. It was proposed that this was the result of the contributions of minor species containing both parallel and anti-parallel loops [16]. In the current work, when Q1 was in 150 mM NH_4OAc but had not been subjected to an annealing step, the maximum at 295 nm decreased and there was a shoulder at ~260 nm and a broad minimum at ~250 nm, suggesting the mixture was heterogeneous. When Q1 was heated to 80 °C or was in 5 mM NH_4OAc with 80% acetonitrile the recognisable features of qDNA in the CD spectra were lost.

The CD spectra of 20 μM Q2 in 5 mM and 150 mM NH_4OAc (Fig. 2(c)) were very similar to that obtained previously in ammonium acetate with a positive maximum at 295 nm and a negative minimum at 260 nm consistent with an anti-parallel strand orientation [27], and both those in the current work and in the literature exhibited a shoulder at ~270 nm. This differs from a CD spectrum of this sequence in the presence of Na^+ in which no shoulder was evident [33]. The shoulder suggests heterogeneity in the structures present in the solutions. An interesting change was noted in the spectrum that related only to the concentration of DNA in the sample. When the concentration was increased to 40 μM, the major features shifted to a maximum at 260 nm and a minimum at 240 nm consistent with conversion to a parallel-stranded qDNA with some residual anti-parallel quadruplex remaining as evidenced by the shoulder at 295 nm. These changes highlight the importance of characterising the solution and annealing conditions for qDNA before using ESI-MS for drug screening.

3.3. Travelling wave ion mobility mass spectrometry of Q4, Q1 and Q2

The mass spectrum and CD of Q4 in 150 mM NH_4OAc (Figs. 1(a), bottom and 2(a), respectively) suggest that the major species present was a parallel four-stranded qDNA in which four ammonium ions were bound within the qDNA structure. In 50 mM NH_4OAc, the ESI mass spectrum showed that the major species now contained three ammonium ions and some single-strands of DNA were present (Fig. 1(a), top). The CD spectrum at an even lower concentration of NH_4OAc (5 mM) was largely unchanged. This suggests that either there was some dissociation in the mass spectrometer or that if single strands were present in 5 mM NH_4OAc, they were not sufficiently abundant to alter the CD spectrum. In order to probe the conformation of electrosprayed qDNA in the gas phase, ion mobility mass spectra were obtained. These are the first travelling wave ion mobility mass spectra of qDNA.

Fig. 3 shows the ESI mass spectra and driftscope images for Q4 sprayed from 150 mM NH_4OAc and from 5 mM NH_4OAc (pH 7.0). The ESI mass spectrum of Q4 acquired using the Synapt ESI-TWIMS was similar to those acquired using the Q-TOF *Ultima* mass spectrometer (Fig. 1(a)), with $[Q4 + 4NH_4^+ - 9H]^{5-}$ the most abundant ion. ESI mass spectra could be acquired using the Synapt ESI-TWIMS instrument using trap and transfer energies of 4 and 2 V, respectively. In order to acquire ion mobility mass spectra, it was necessary to increase the trap and transfer energies to 6 and 3 V, respectively. These were the conditions used to acquire all ion mobility mass spectra reported in this work and are the conditions applied to produce the spectra shown in Figs. 3–5. The ion $[Q4 + 4NH_4^+ - 9H]^{5-}$ (labelled **b** in Fig. 3(b)) remained the most abundant, but $[Q4 + 3NH_4^+ - 8H]^{5-}$ increased to approximately two-thirds of the abundance of the former ion. The ion mobilities (arrival times in ms) were determined by taking the peak of intensity for each ion from the driftscope plot showing the arrival time distribution (not shown). Table 2 shows the calculated and observed *m*/*z* values for ions, their arrival times and their assignment. The assignment of ions was relatively straightforward in the case of Q4 with the appearance of ions from ssDNA (labelled **f** and **g** in Fig. 3(c) and (d)) in 5 mM NH_4OAc. The only ion where the assignment is ambiguous from analysis of the ESI mass spectrum alone is ion **e** ($[Q4 + 4NH_4^+ - 12H]^{8-}$) in Fig. 3(d) which could also be assigned as $[ssQ4 + NH_4^+ - 3H]^{2-}$ (where ssQ4 refers to a single strand). The driftscope image (Fig. 3(c)) shows that this ion is diagonally aligned with the series (ions **b**–**d**) corresponding to Q4 with four bound ammonium ions supporting that ion **e** is $[Q4 + 4NH_4^+ - 12H]^{8-}$. There were some ions of very low abundance (not labelled) that were consistent with the loss of a guanine base(s)

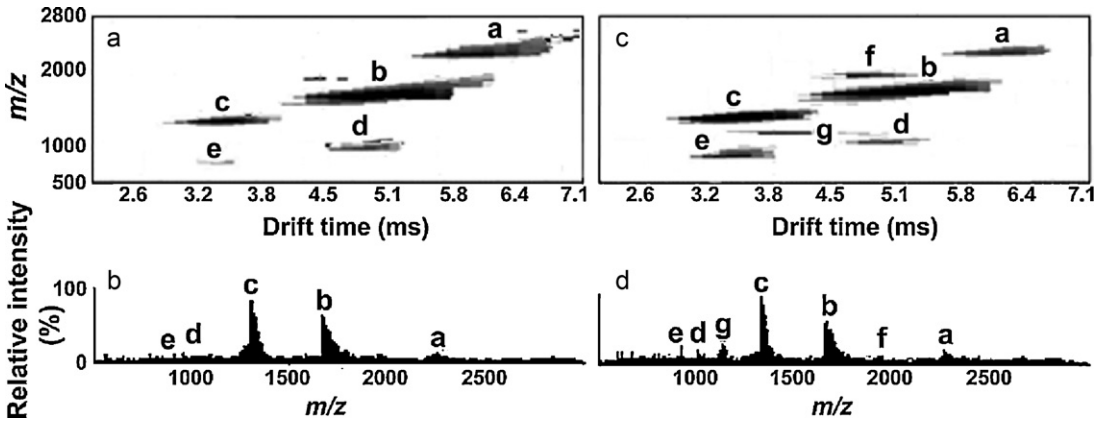

Fig. 4. Negative ion ESI mass spectra and TWIMS driftscope images of Q1. (a), (b) In 150 mM NH_4OAc. (c), (d) In 5 mM NH_4OAc. The ions from intact Q1 are **b**, **c** and **g** which correspond to $[Q1\text{-}4H]^{4-}$, $[Q1\text{-}5H]^{5-}$ and $[Q1\text{-}6H]^{6-}$, respectively. All ions are assigned in Table 3.

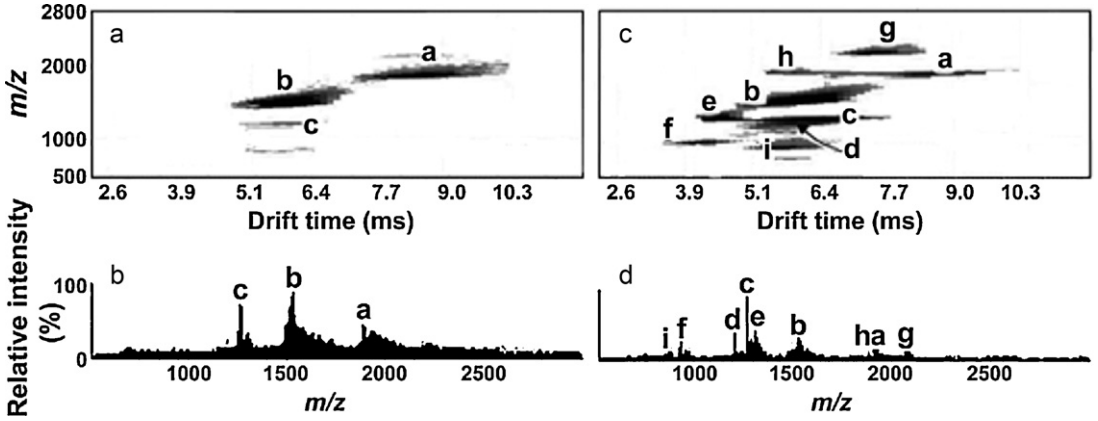

Fig. 5. Negative ion ESI mass spectra and TWIMS driftscope images of Q2. (a), (b) In 150 mM NH_4OAc. (c), (d) in 5 mM NH_4OAc, 40% in acetonitrile. The ions from intact Q2 are **a**, **b** and **e** which correspond to $[Q2\text{-}4H]^{4-}$, $[Q2\text{-}5H]^{5-}$ and $[Q2\text{-}6H]^{6-}$, respectively. All ions are assigned in Table 4.

most likely from the DNA (*e.g.*, $[Q4 + 4NH_4^+ - 2G\text{-}9H]^{5-}$ at *m/z* 1949.5). An expanded view of the *m/z* range 1940–2015 is shown in the supplementary material (Fig. S1). When Q4 was sprayed from 5 mM NH_4OAc, 40% in acetonitrile (not shown), the ESI mass spectrum and driftscope image was similar to those observed for 5 mM NH_4OAc alone, but the abundance of all ions was greater, most likely as a result of enhanced desolvation when the solvent was present.

The ESI mass spectrum of Q1 acquired using the Synapt TWIMS (trap and transfer at 4 and 2 V, respectively) was similar to that obtained using the Q-TOF *Ultima* with K^+ and/or Na^+ adducts evident. In order to acquire ion mobility mass spectra the trap energy was increased as described for Q4 (Table 1). Fig. 4 shows the ESI mass spectra and driftscope images for Q1 sprayed from 150 and 5 mM NH_4OAc. Table 3 shows the assignment of all ions in Fig. 4. The ESI mass spectrum in 150 mM NH_4OAc (Fig. 4(b)) shows that

Table 2
Assignment of ions for ESI-TWIMS of Q4 (Fig. 3).

Label	Observed *m/z*	Calculated *m/z*	Arrival time (ms)[a]	Assignment
150 mM NH_4OAc, pH 7.0				
a	2512.6	2512.8	12.8	$[Q4 + 4NH^{4+} - 8H]^{4-}$
b	2009.8	2010.0	8.2	$[Q4 + 4NH^{4+} - 9H]^{5-}$
c	1674.4	1674.8	5.8	$[Q4 + 4NH^{4+} - 10H]^{6-}$
5 mM NH_4OAc, pH 7.0				
b	2009.8	2010.0	8.2	$[Q4 + 4NH^{4+} - 9H]^{5-}$
c	1674.4	1674.8	5.8	$[Q4 + 4NH^{4+} - 10H]^{6-}$
d	1435.0	1435.4	4.6	$[Q4 + 4NH^{4+} - 11H]^{7-}$
e	1256.2	1256.4	3.8	$[Q4 + 4NH^{4+} - 12H]^{8-}$
f	1247.3	1247.3	7.7	$[ssQ4\text{-}2H]^{2-}$
g	831.1	831.2	4.4	$[ssQ4\text{-}3H]^{3-}$
h[b]	974.1	ND	6.2	ND

ND = not determined.
[a] The ion mobilities were determined by taking the peak of intensity for each ion from the driftscope plot showing the arrival time distribution (not shown).
[b] This ion was observed in 5 mM NH_4OAc but is not labelled in Fig. 3. It was present in higher abundance when acetonitrile was present (supplementary Fig. S2).

Table 3
Assignment of ions for ESI-TWIMS of Q1 (Fig. 4).

Label	Observed *m/z*	Calculated *m/z*	Arrival time (ms)[a]	Assignment
150 mM NH_4OAc, pH 7.0				
a	2216–2300[b]	2216.8	6.4	$[2{\cdot}Q1\text{-}6H]^{6-}$
b	1662.5	1662.3	5.1	$[Q1\text{-}4H]^{4-}$
c	1330.0	1329.7	3.5	$[Q1\text{-}5H]^{5-}$
5 mM NH_4OAc, pH 7.0				
a	2216–2300[b]	2216.8	6.4	$[2{\cdot}Q1\text{-}6H]^{6-}$
b	1662.5	1662.3	5.1	$[Q1\text{-}4H]^{4-}$
c	1330.0	1329.7	3.5	$[Q1\text{-}5H]^{5-}$
d	920–930[b]	922.6	5.1	Fragments including y_6^{2-}
e	700–780[b]	770.5	3.5	Fragments including y_4^{2-}
f	1900–1960[c]	1900.0	4.8	$[2{\cdot}Q1\text{-}7H]^{7-}$
g	1108.0	1107.9	3.8	$[Q1\text{-}6H]^{6-}$

[a] The ion mobilities were determined by taking the peak of intensity for each ion from the driftscope plot showing the arrival time distribution (not shown).
[b] Range given because there were numerous adducts to higher *m/z* and the ion at calculated *m/z* was present in low abundance in the ESI mass spectrum.
[c] Difficult to assign as numerous ions at low abundance are present in this region.

the abundance of $[Q1\text{-}5H]^{5-}$ (ion **c**) at *m/z* 1329.7 was increased (*cf.* Fig. 1(b)), and very low abundance ions at around *m/z* 920–930 and 700–780 appeared. In these regions two ions of relatively narrow peak width were observed (labelled **d** and **e** at *m/z* 922.1 and 770.4, respectively). A cursory inspection of the driftscope image (Fig. 4(a)), suggests that ions **a**–**c** might be assigned as the $[Q1\text{-}3H]^{3-}$, $[Q1\text{-}4H]^{4-}$ and $[Q1\text{-}5H]^{5-}$ ions. The assignment of ion **a** will be revisited below. Based on the driftscope image, the ions **d** and **e** clearly are not in diagonal alignment with **a**–**c**, so represent a different structure. These ions do not correspond to any calculated ion from an intact strand of Q1 and represent fragmentation of the DNA under the mass spectrometry conditions. The calculated *m/z* values for the y_6^{2-} and y_4^{2-} ions are 922.6 and 770.5, respectively, and these are consistent with ions **d** and **e**. When Q1 was sprayed from 5 mM NH_4OAc, ions **f** (*m/z* 1900.0) and **g** (*m/z* 1107.9) were present at low abundance (Fig. 4(c) and (d)). The calculated *m/z* for $[Q1\text{-}6H]^{6-}$ is 1107.9. If ion **g** were to be assigned on the basis of the mass spectrum alone, it would appear that Q1 in 5 mM NH_4OAc exhibited the $[Q1\text{-}4H]^{4-}$ (ion **b**), $[Q1\text{-}5H]^{5-}$ (ion **c**) and $[Q1\text{-}6H]^{6-}$ (ion **g**). This proposal is apparently supported by the CD spectrum of Q1 (Fig. 2(b)) which was unchanged when the NH_4OAc concentration was decreased from 150 to 5 mM. This assignment is, however, unlikely since the ion mobility shows that ion **g** is not aligned with ions **b** and **c**, suggesting that $[Q1\text{-}6H]^{6-}$ (ion **g**) occurs when Q1 is unfolded with no defined secondary structure. Since ion **g** was not present when Q1 was sprayed from 150 mM NH_4OAc but was present when Q1 was in 5 mM NH_4OAc, this suggests that the unfolding occurred in solution. While this is not evident from the CD spectra, the mass spectrum (Fig. 4(d)) shows that the unfolded DNA (ion **g**) is not very abundant. This observation shows the utility of ESI-TWIMS in this case for detecting the conditions under which the qDNA becomes less stable and also supports that TWIMS has the ability to resolve folded and unfolded Q1.

The position of ion **f** in the driftscope image (Fig. 4(c)) suggests that it is from a structure common with ion **a**. The previous tentative assignment for ion **a** was $[Q1\text{-}3H]^{3-}$. Another ion with the same *m/z* value is $[2{\cdot}Q1\text{-}6H]^{6-}$ (indicating a dimer of Q1). Previously, using a much shorter sequence, Balasubramanian and coworkers showed that d(GGGT) could form qDNA, $(dGGGT)_4$, and an interlocked dimer $(dGGGT)_8$. In this dimeric structure "slippage" results in the overhang of two guanine bases that are not involved in the qDNA tetrads. Two slipped qDNA molecules dimerise via these free bases to form an extra G-tetrad stabilising the dimer [34]. The calculated *m/z* value for $[2{\cdot}Q1\text{-}7H]^{7-}$ is 1900.0 and this is consistent with ion **f**. The presence of two ions consistent with this structure lends support to, but does not confirm these assignments. Ion **f** was present at very low abundance in all ESI mass spectra, but was readily observable in the driftscope image. Its precise *m/z* value was difficult to determine as a consequence of its low abundance and the presence of associated ions from adducts. It is not possible to confirm whether the proposed dimer (or other structure) was present in solution or occurred as a result of the ionisation process (association of two monomers in a droplet at the final stages of the ionisation process). The presence of a dimer in solution might account for the heterogeneity suggested by CD spectra of a similar qDNA sequence [16].

Ion **g** has been assigned as $[Q1\text{-}6H]^{6-}$ and is consistent with unfolded Q1. Support for this suggestion was found when Q1 was sprayed from 5 mM NH_4OAc, 40% in acetonitrile (supplementary material, Fig. S2): an ion **h** at *m/z* 949.5 appeared, consistent with (unfolded) $[Q1\text{-}7H]^{7-}$. In the ESI mass spectrum of this sample, the most abundant ion was ion **g** consistent with unfolding of the qDNA structure as the percentage of organic solvent was increased. In addition, ions of low abundance were present below *m/z* 900. These were not assigned but are likely to represent fragmentation of Q1. Since these ions appeared as unfolded qDNA became more abundant, this suggests that Q1 was protected against fragmentation when it was present in its folded form.

Table 4
Assignment of ions for ESI-TWIMS of Q2 (Fig. 5).

Label	Observed *m/z*	Calculated *m/z*	Arrival time (ms)[a]	Assignment
150 mM NH_4OAc, pH 7.0				
a	1893.0	1893.2	8.4	$[Q2\text{-}4H]^{4-}$
b	1515.0	1514.4	5.6	$[Q2\text{-}5H]^{5-}$
c	1262.1	1261.8	5.7	$[ssQ2\text{-}3H]^{3-}$
5 mM NH_4OAc, pH 7.0, 40% in acetonitrile				
a	1893.0	1893.2	8.4	$[Q2\text{-}4H]^{4-}$
b	1515.0	1514.4	5.6	$[Q2\text{-}5H]^{5-}$
c	1262.1	1261.8	5.7	$[ssQ2\text{-}3H]^{3-}$
d	1210.8	1211.5	5.5	$[ssQ2\text{-}3H\text{-}G]^{3-}$
e	1262.0	1261.8	4.4	$[Q2\text{-}6H]^{6-}$
f	946.0	946.1	3.6	$[ssQ2\text{-}4H]^{4-}$
g	2160–2200[b]	2163.9	7.4	$[2{\cdot}Q2\text{-}7H]^{7-}$
h	1890–1950[b]	1893.2	5.8	$[2{\cdot}Q2\text{-}8H]^{8-}$
i	850–1000[b]	ND[c]	5.8	Fragments[c]

ND = not determined.
[a] The ion mobilities were determined by taking the peak of intensity for each ion from the driftscope plot showing the arrival time distribution (not shown).
[b] Range given because there were numerous adducts to higher *m/z* and the ion at calculated *m/z* was present in low abundance in the ESI mass spectrum.
[c] Difficult to assign as numerous ions at low abundance are present in this region.

Fig. 5 shows the ESI mass spectra and driftscope images of Q2 sprayed from 150 mM NH_4OAc and from 5 mM NH_4OAc, 40% in acetonitrile (note for Q4 and Q1, the solutions shown were 150 and 5 mM NH_4OAc). The ESI mass spectrum of Q2 in 150 mM ammonium acetate obtained using the ESI-TWIMS was similar to that obtained using the Q-TOF *Ultima* except that an ion at *m/z* 1261.8 (ion **c** in Fig. 5(b)) was abundant. In addition, $[Q2\text{-}4H]^{4-}$ (**a** at *m/z* 1893.2) and $[Q2\text{-}5H]^{5-}$ (**b** at *m/z* 1514.4) were abundant. Associated ions arising from adducts with bound ammonium ions were still present, but were less abundant than Q2 alone. This suggests that under the less gentle conditions required to obtain ion mobility mass spectra that ammonium ions were lost from the structure. The ammonium adducts can still be observed in the mass spectra; for example, note the adducts (to higher *m/z*) associated with ions **a** and **b** in the mass spectra (Fig. 5(b) and (d)). Table 4 shows the assignment of the ions to lower *m/z* (no adducts) but does not include the adducted ions which were of lower abundance under the conditions used to obtain ion mobility mass spectra than when ESI mass spectra alone (lower trap and transfer energies) were acquired. Ion **c** corresponds to a single strand of Q2 carrying three negative charges and will be referred to as $[ssQ2\text{-}3H]^{3-}$. Note that this ion has a narrow peak width and is not associated with any adducts. The presence of this ion at the same arrival time as $[Q2\text{-}5H]^{5-}$ supports that some of the bimolecular Q2 qDNA was unfolded in the mass spectrometer, possibly the result of destabilisation through loss of ammonium ions under the conditions in the ESI-TWIMS.

When Q2 was sprayed from 5 mM NH_4OAc (not shown), ions **d**, **e** and **f** appeared. In the presence of 5 mM NH_4OAc, 40% in acetonitrile (Fig. 5(c)), ions **h** and **i** appeared. The ion **h** occurs at the same *m/z* 1893 as ion **a** which was assigned as $[Q2\text{-}4H]^{4-}$ but clearly has a different arrival time. Ion **h** therefore arises from a structure other than the folded bimolecular qDNA structure proposed for Q2 on the basis of the similarity of the CD spectra to those observed in other work and on X-ray crystal structures. Possible candidates are some other conformation of $[Q2\text{-}4H]^{4-}$ that is resolvable by TWIMS, $[ssQ2\text{-}2H]^{2-}$ and $[2{\cdot}Q2\text{-}8H]^{8-}$. $[ssQ2\text{-}3H]^{3-}$ has already been proposed for ion **c**. Reference to the driftscope image shows that ions **c** and **h** are not diagonally aligned and argues against the identity of **h** as $[ssQ2\text{-}2H]^{2-}$. The assignment of ion **h** will be revisited below. Ion **e** at *m/z* 1262.0 corresponds to $[Q2\text{-}6H]^{6-}$ (calculated *m/z* 1261.8, no

bound ammonium ions). This is the same m/z calculated for [ssQ2-3H]$^{3-}$. The different arrival times of ion **e** (4.4 ms) and ion **c** (5.7 ms) support these assignments. The diagonal alignment with ions **a** and **b** suggests that **e** corresponds to folded bimolecular Q2 qDNA. It is possible that ammonium ions were lost in the gas phase but this structure remains intact. In previous work it was also not possible to observe ammonium ions bound to Q2 except under very gentle conditions using a Q-TOF2 mass spectrometer [27]. Ions **d** and **c** occur at approximately the same arrival time (see Fig. 5(c)) and **d** at m/z 1210.8 is consistent with [ssQ2-3H-G]$^{3-}$ (calculated m/z 1211.5) arising from dissociation of guanine from **c** ([ssQ2-3H]$^{3-}$). This is consistent with unfolded, single-strands of DNA being less stable to fragmentation of the glycosidic bonds under the mass spectrometry conditions. Brodbelt and coworkers have previously observed in ESI-MS/MS experiments that Q2 dissociates primarily via guanine base loss with some strand dissociation [35]. Ion **f** occurs at m/z 946.1 and corresponds to [ssQ2-4H]$^{4-}$ and its diagonal alignment with **c** supports this assignment. Since the single strands were not present when Q2 was sprayed from 150 mM NH_4OAc, this suggests that the mass spectrometry conditions were sufficiently gentle under those conditions to maintain the bimolecular qDNA structure of Q2.

Ion **g** was present at low abundance when Q2 was sprayed from 150 mM NH_4OAc but is not labelled in Fig. 5(a) and was also present at low abundance when Q2 was in 5 mM ammonium acetate (no acetonitrile). When Q2 was sprayed from 5 mM NH_4OAc, 40% in acetonitrile (Fig. 5(c)), ion **g** increased in abundance. The arrival time of ion **g** suggests that it corresponds to a structure that is different from the bimolecular Q2 qDNA (*cf.* arrival times of ions **a** and **b**). Ion **g** is associated with adducts (m/z 2160–2200) that are difficult to assign unequivocally as a consequence of their low abundance, but their presence suggests some kind of secondary structural elements. The ion [2·Q2-7H]$^{7-}$ has a calculated m/z value of 2163.9. The presence of a dimer would be consistent with the different mobility observed for ion **g**, with the presence of numerous adducts and with the tentative assignment of ion **h** as [2·Q2-8H]$^{8-}$. The increase in abundance of ions from the dimer in the presence of acetonitrile may be the result of enhanced desolvation of this species. Ion **i** and other very low abundance ions in this region of the mass spectrum do not correspond to intact DNA and arise from fragmentation in the mass spectrometer. Given the observation of interlocked dimers that occur for $(dGGGT)_4$ discussed above [34], it is feasible that Q2 $(dG_4T_4G_4)_2$ could also form dimers if slipped structures are present. The CD spectra of Q2 revealed that when the Q2 concentration was increased that the qDNA changed from a mixture where an anti-parallel strand orientation was predominant to a mixture where Q2 in a parallel strand orientation was also present. Since oligomers such as dimers would be favoured by the higher concentrations, it can be speculated that the dimers tentatively assigned in the mass spectrum might be the source of the parallel qDNA structures suggested by the CD spectra.

4. Conclusions

This is the first report of ESI-TWIMS of qDNA. The ion mobilities observed were related to known structures determined for these and similar qDNA sequences using NMR and X-ray crystallography. Support for the maintenance of folded qDNA in the gas phase was obtained by changing the solution conditions to destabilise qDNA structures, obtaining ion mobility mass spectra and comparing the driftscope images (arrival times of ions) with those previously obtained. In some cases, ions of the same m/z but very different arrival times were observed. This enabled distinction among bimolecular qDNA (Q2) and its single strands (ions **c** and **e** which were assigned as [ssQ2-3H]$^{3-}$ and [Q2-6H]$^{6-}$, respectively). The presence of the dimer may account for changes observed in the CD spectra of Q2 at high concentrations. The resolution of the ESI-TWIMS was sufficient to be able to distinguish among folded Q1 (an intramolecular qDNA) and its unfolded form (ion **g** proposed as unfolded [Q1-6H]$^{6-}$), as it appeared only at lower ionic strength, was abundant when acetonitrile was present and does not align with ions **b** and **c** (proposed as [Q1-4H]$^{4-}$ and [Q1-5H]$^{5-}$, respectively, from folded Q1). It would not have been possible to distinguish among the folded and unfolded structures using ESI-MS alone or by reference to the CD spectrum. Previously, single-molecule spectroscopy has shown that human telomeric DNA exists in a number of conformational forms [36].

This study illustrates the utility of ESI-TWIMS for analysis of qDNA. This is particularly important when ESI-MS is to be used to screen the binding of ligands to the DNA as false positive or false negative results might be obtained if the qDNA sample is significantly heterogeneous. This work has served as a starting point for analysis of the binding of berberine derivatives to various qDNA structures in an extension of our previous work [25]. In these studies to be reported elsewhere, the solution and gas phase stabilities of qDNA was enhanced when the ligands were bound.

Acknowledgements

We wish to thank the University of Wollongong, Australia, for supporting this work. The award of an APA scholarship (K. Porter) is also gratefully acknowledged, together with support from the Centre for Medical Bioscience, University of Wollongong. We also thank the Australian Research Council for the mass spectrometers used in this work.

Appendix A. Supplementary data

Supplementary data associated with this article can be found, in the online version, at doi:10.1016/j.ijms.2010.10.033.

References

[1] J.D. Watson, F.H. Crick, Nature 171 (1953) 737.
[2] J.L. Beck, T. Urathamakul, S.J. Watt, M.M. Sheil, P.M. Schaeffer, N.E. Dixon, Expert Rev. Proteomics 3 (2006) 197.
[3] R.D. Wells, Trends Biochem. Sci. 32 (2007) 271.
[4] S. Balasubramanian, S. Neidle, Curr. Opin. Chem. Biol. 13 (2009) 345.
[5] M.A. Keniry, Biopolymers 56 (2001) 123.
[6] S.M. Kerwin, Curr. Pharm. Des. 6 (2000) 441.
[7] M.-Y. Kim, M. Gleason-Guzman, E. Izbicka, D. Nishioka, L.H. Hurley, Cancer Res. 63 (2003) 3247.
[8] W.E. Wright, V.M. Tesmer, K.E. Huffman, S.D. Levene, J.W. Shay, Genes Dev. 11 (1997) 2801.
[9] R.K. Moyzis, J.M. Buckingham, L.S. Cram, M. Dani, L.L. Deavan, M.D. Jones, J. Meyne, R.L. Ratliff, J.R. Wu, Proc. Natl. Acad. Sci. U.S.A. 85 (1988) 6622.
[10] D.J. Slamon, J.B. deKernion, I.M. Verma, M.J. Kline, Science 224 (1984) 256.
[11] A.T. Phan, V. Kuryavyi, H.Y. Gaw, D.J. Patel, Nat. Chem. Biol. 1 (2005) 167.
[12] N.W. Kim, M.A. Piatyszek, K.R. Prowse, C.B. Harley, M.D. West, P.L. Ho, G.M. Coviello, W.E. Wright, S.L. Weinrich, J.W. Shay, Science 266 (1994) 2011.
[13] S. Neidle, G.N. Parkinson, Biochimie 90 (2008) 1184.
[14] M. Lu, Q. Guo, N.R. Kallenbach, Biochemistry (1993) 598.
[15] R. Giraldo, M. Suzuki, L. Chapman, D. Rhodes, Proc. Natl. Acad. Sci. U.S.A. 91 (1994) 7658.
[16] E. Shammel Baker, S.L. Bernstein, V. Gabelica, E. de Pauw, M.T. Bowers, Int. J. Mass Spectrom. 253 (2006) 225.
[17] J.L. Beck, M.L. Colgrave, S.F. Ralph, M.M. Sheil, Mass Spectrom. Rev. 20 (2001) 61.
[18] S.E. Pierce, R. Kieltyka, H.F. Sleiman, J.S. Brodbelt, Biopolymers 91 (2009) 233.
[19] G. Collie, A.P. Reszka, S.M. Haider, V. Gabelica, G.N. Parkinson, S. Neidle, Chem. Commun. 48 (2009) 7482.
[20] A.B. Kanu, P. Dwivedi, M. Tam, L. Matz, H.H. Hill, J. Mass Spectrom. 43 (2008) 1.
[21] V. Gabelica, E. Shammel Baker, M.-P. Teulade-Fichou, E. de Pauw, M.T. Bowers, J. Am. Chem. Soc. 129 (2007) 895.
[22] T. Wyttenbach, P.R. Kemper, M.T. Bowers, Int. J. Mass Spectrom. 212 (2001) 13.
[23] S.D. Pringle, K. Giles, J.L. Wildogoose, J.P. Williams, S.E. Slade, K. Thalassinos, R.H. Bateman, M.T. Bowers, J.H. Scrivens, Int. J. Mass Spectrom. 261 (2007) 1.
[24] D.P. Smith, T.W. Knapman, I. Campuzano, R.W. Malham, J.T. Berryman, S.E. Radford, Eur. J. Mass Spectrom. 15 (2009) 113.

[25] K.C. Gornall, S. Samosorn, J. Talib, J.B. Bremner, J.L. Beck, Rapid Commun. Mass Spectrom. 21 (2007) 1759.
[26] K.C. Gornall, S. Samosorn, B. Tanwirat, A. Suksamrarn, J.B. Bremner, M.J. Kelso, J.L. Beck, Chem. Commun. 46 (2010) 6602.
[27] F. Rosu, V. Vabelica, C. Houssier, P. Colson, E. de Pauw, Rapid Commun. Mass Spectrom. 16 (2002) 1729.
[28] W.M. David, J. Brodbelt, S.M. Kerwin, P.W. Thomas, Anal. Chem. 74 (2002) 2029.
[29] G.N. Parkinson, M.P.H. Lee, S. Neidle, Nature 417 (2002) 876.
[30] Y. Wang, D.J. Patel, Structure 1 (1993) 263.
[31] Y. Xue, A. Kan, Q. Wang, Y. Yao, J. Liu, T. Hao, Z. Tan, J. Am. Chem. Soc. 129 (2007) 11185.
[32] S. Haider, G.N. Parkinson, S. Neidle, J. Mol. Biol. 326 (2003) 117.
[33] P. Balagurumoorthy, S.K. Brahmachari, D. Mohanty, V. Sasisekharan, Nucleic Acids Res. 20 (1992) 4061.
[34] Y. Krishnan-Ghosh, D. Liu, S. Balasubramanian, J. Am. Chem. Soc. 126 (2004) 11009.
[35] C.L. Mazzitelli, J. Wang, S.I. Smith, J.S. Brodbelt, J. Am. Soc. Mass Spectrom. (2007) 1760.
[36] J.Y. Lee, B. Okumas, D.S. Kim, T. Ha, Proc. Natl. Acad. Sci. U.S.A. 102 (2005) 18938.